INSTITUTE OF PHYSICS PUBLISHING JOURNAL OF PHYSICS: CONDENSED MATTER

J. Phys.: Condens. Matter **16** (2004) 1425–1437 PII: S0953-8984(04)67568-0

A classical model for the magnetic field-induced Wigner crystallization in quantum dots

T Prus, B Szafran, J Adamowski and S Bednarek

Faculty of Physics and Nuclear Techniques, AGH University of Science and Technology, aleja Mickiewicza 30, PL-30059 Kraków, Poland

E-mail: bszafran@agh.edu.pl

Received 14 August 2003
Published 13 February 2004
Online at stacks.iop.org/JPhysCM/16/1425 (DOI: 10.1088/0953-8984/16/8/023)

Abstract

A classical model is presented for magnetic field-induced Wigner crystallization in electron systems confined within two-dimensional quantum dots. In contrast to other classical models, this one does not treat an electron as a point charge; the electron density is assumed to take a Gaussian form corresponding to the lowest Landau level. Using a Monte Carlo method we have determined the equilibrium configurations as functions of the magnetic field. We have found a classical counterpart of the quantum maximum density droplet (MDD) and studied the breakdown of the MDD into a Wigner molecule as well as the transformations of the Wigner molecule shape induced by the external magnetic field. The phase diagram for the classical Wigner molecules has been presented and its qualitative agreement with previous quantum mechanical calculations has been shown.

1. Introduction

In the strongly correlated bulk systems, the electrons can be localized at distinct lattice sites forming a Wigner crystal [1]. In quantum dots which do not possess translational symmetry, states with island-like electron localization, called Wigner molecules [2–9, 12–17] are formed. At high magnetic field the quantum charge density distribution in the inner coordinates becomes classical [8]. For this reason the classical theory of Wigner crystallization has become of significant interest over the last decade [18–27]. In particular, the influence of the form of the confinement and interaction potentials on the symmetry of the confined classical system has been studied [23]. Recently, an experimental study [28] has been performed in order to find equilibrium configurations in millimetre-sized charged-ball systems.

The quantum electron system confined in a quantum dot and subject to an external magnetic field has been studied in a number of theoretical papers [2–9, 11, 12, 29–34]. Much of the theoretical interest has been aroused by the experimental observation [35] of the decay of the maximum density droplet (MDD) [29]. The MDD is the phase which appears when all the electrons become spin polarized by the external magnetic field. In the MDD phase, the electrons occupy the lowest energy Fock–Darwin states (corresponding to the lowest Landau

level [8]). The MDD possesses a characteristic single flat maximum of the charge density distribution. At sufficiently high magnetic field the MDD decays, i.e., is replaced by a state with higher angular momentum. The MDD can be quite accurately described by the restricted Hartree–Fock method [11, 29], which means that the electron–electron correlation is of secondary importance in this phase. On the other hand, the ground state, which appears at higher magnetic fields after the MDD decay, is strongly correlated. The spatial separation of the electrons in high magnetic fields leads to the formation of Wigner molecules [2–9]. In the infinite magnetic field limit, the system becomes classical, i.e., the energy [6] and the charge distribution can be obtained from the classical physics.

The transformations of the electron charge density distribution have become a subject of study recently [7, 9, 31, 32]. Reimann *et al* [7] studied the edge reconstruction in vertical quantum dots using spin density functional theory. Manninen *et al* [31] investigated a system of six electrons using the exact diagonalization method. The authors of [8, 31] found that the Wigner molecule which is created after the MDD breakdown corresponds to the electrons forming a hegaxon. At higher magnetic fields this configuration is transformed into a configuration with one electron at the centre and five other electrons forming a pentagon. This result was qualitatively confirmed by Yang and MacDonald [32], who addressed the problem of the occupation of the single-particle angular momentum eigenstates using exact diagonalization. The authors of [32] found that for less than 14 electrons the charge density spatial distribution obtained after the MDD decay has a hole at the centre of the dot. This hole is filled in higher magnetic fields. This effect was also found by Szafran *et al* [9], who studied the transformations of the ground state spatial symmetry of Wigner molecules in the magnetic field regime between the MDD and the classical high magnetic field limit using the multicentre Hartree–Fock method, i.e., the Hartree–Fock method with the basis functions corresponding to the lowest Landau level centred around different sites.

The two-electron problem possesses analytical solutions for certain oscillator frequencies [36]. A number of exact numerical results for few-electron systems have also been published [11, 12, 30–32]. In this paper we do not solve the many-electron problem by quantum mechanical means, but reduce it to a form amenable to treatment by the methods of classical physics. For this purpose we have introduced an electron–electron interaction potential derived from the assumption that the electrons occupy the lowest Landau level only. Accordingly, the charge density distribution of the single electron is taken as a Gaussian function corresponding to the lowest Landau level. In the following, we will show that not only the high magnetic field behaviour but also some of the most characteristic features of the quantum systems under finite magnetic fields can be obtained in the framework of classical physics. In particular we show that the present classical approach reproduces the MDD decay into the Wigner molecule and the phase transitions (shape transformations) of the Wigner molecules induced by the external magnetic field. Since the present approach accounts only for the classical potential energy, it implies that these effects can be qualitatively explained without making reference to the purely quantum exchange and correlation energy contributions. On the other hand, for this reason the present approach should not be expected to give quantitative agreement with exact or approximate quantum calculations for an arbitrary value of the magnetic field.

The paper is organized as follows: section 2 contains the theory; the results and discussion are presented in section 3; and section 4 contains the conclusions and summary.

2. Theory

We consider a system of N electrons confined in the two-dimensional (2D) quantum dot and subject to an external magnetic field. In a high magnetic field the influence of the confinement

potential is of secondary importance and the occupied one-electron states can be identified with the degenerate lowest energy Landau state. The ground state wavefunction, written in the Landau gauge, has the form [9]

$$\psi_{\mathbf{R}}(\mathbf{r}) = (\alpha/2\pi)^{1/2} \exp[-(\alpha/4)(\mathbf{r}-\mathbf{R})^2 + (\mathrm{i}\alpha/2)(x-X)(y+Y)], \tag{1}$$

where $\mathbf{r} = (x, y)$, the charge density centre position $\mathbf{R} = (X, Y)$ is an arbitrary point on the x–y plane, $\alpha = eB/\hbar$, B stands for the magnetic field, and $e > 0$ stands for the elementary charge. The charge density of the electron described by wavefunction (1) is given by

$$\varrho_{\mathbf{R}}(\mathbf{r}) = -e(\alpha/2\pi) \exp[-(\alpha/2)(\mathbf{r}-\mathbf{R})^2]. \tag{2}$$

In the limit of infinite magnetic field, $\varrho_{\mathbf{R}}(\mathbf{r})$ becomes the point charge distribution.

We assume that the electrons are confined in the harmonic oscillator potential $V_{\mathrm{conf}}(r) = m\omega_0^2 r^2/2$, where m is the effective mass of the electron and ω_0 is the confinement frequency. The potential energy of the single electron with charge distribution (2) in an external field $V_{\mathrm{conf}}(r)$ is calculated as follows:

$$\int \mathrm{d}^2 r\, V_{\mathrm{conf}}(\mathbf{r}) \frac{\varrho_{\mathbf{R}}(\mathbf{r})}{(-e)} = V_{\mathrm{conf}}(R) + m\omega_0^2/\alpha. \tag{3}$$

In equation (3), the first term is independent of α, i.e., magnetic field B, and is the same as for the point charge, while the second term is independent of $\mathbf{R}$, i.e., has no influence on the equilibrium configuration of the Wigner molecule. Therefore, in the calculations, we neglect the second term. The total potential energy of the N-electron system is a sum of the external potential energy and the interaction energy, i.e.,

$$E_{\mathrm{pot}} = \sum_{i=1}^{N} \left(V_{\mathrm{conf}}(\mathbf{R}_i) + \sum_{j>i}^{N} W(|\mathbf{R}_i - \mathbf{R}_j|, B) \right). \tag{4}$$

The potential energy of the electron–electron interactions is equal to the Hartree energy for the fixed Landau radius and is given by

$$W(|\mathbf{R}_i - \mathbf{R}_j|, B) = \int \mathrm{d}^2 r_1\, \mathrm{d}^2 r_2\, \varrho_{\mathbf{R}_i}(\mathbf{r}_1) \varrho_{\mathbf{R}_j}(\mathbf{r}_2) \frac{\kappa}{|\mathbf{r}_1 - \mathbf{r}_2|}, \tag{5}$$

where $\kappa = 1/4\pi\varepsilon_0\varepsilon$ and ε is the dielectric constant. The interaction energy (5) can be calculated from the integral

$$W(R, B) = \frac{\kappa e^2}{2} \sqrt{\frac{\alpha}{\pi}} \int_0^{\pi} \mathrm{d}\phi\, \exp\left(-\frac{\alpha R^2 \sin^2\phi}{4} \right) \mathrm{erfc}\left(\frac{\sqrt{\alpha} R \cos\phi}{2} \right). \tag{6}$$

Figure 1 displays interaction energy (6) calculated for different magnetic fields and—for comparison—the Coulomb potential energy of the interaction between the point charges ($e^2\kappa/R$). In contrast to the Coulomb potential, interaction energy (6) is finite for $R = 0$. Its maximum value at $R = 0$ increases with increasing magnetic field. Figure 1 shows that the potential energy of the interaction between the Gaussian charge density distributions becomes larger than the Coulomb potential energy at some interelectron distance. If distance R grows, W converges to the Coulomb potential energy. This convergence is faster for the higher magnetic fields, for which the Gaussian charge density begins to resemble that of the point charges.

In quantum calculations the width of the Gaussian wavefunctions is often used as a variational parameter [6, 9, 10, 37] (a detailed discussion of the dependence of this parameter on the magnetic field for Wigner molecules is given in [10]). However, this approach is not applicable to the present classical model. In the quantum mechanical approach the kinetic energy contribution ensures a finite spread of the single-electron wavefunctions. Minimizing

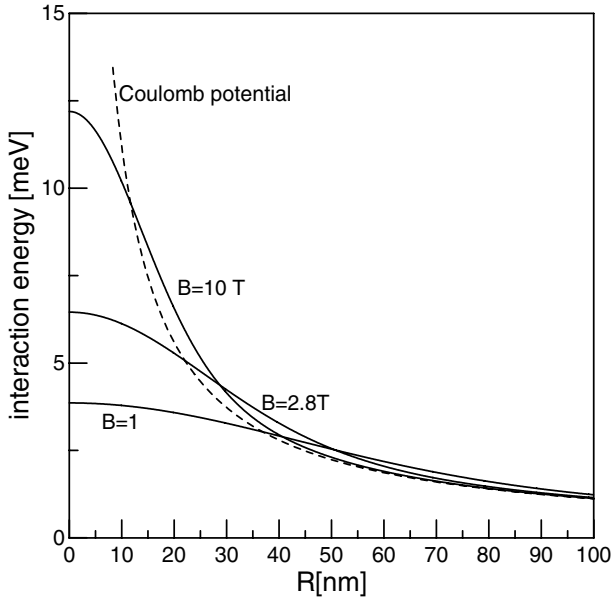

Figure 1. The potential energy (6) of the interaction between the Gaussian charge densities for different magnetic fields B and the Coulomb potential energy as functions of the distance R between the charge density centres.

the classical energy with respect to α would usually lead to a collapse of the single-electron charge density to the delta-like point charge distribution. In the present paper the fixed value of parameter α accounts for the external magnetic field and the finite extent of the electron charge density.

The calculations have been performed for systems of $N = 2, \ldots, 20$ electrons with $m = 0.067\ m_e$ and $\varepsilon = 12.9$, which corresponds to GaAs. We consider the lateral confinement energy $\hbar\omega_0 = 3$ meV, which allows us to address the quantum system studied in [2, 9, 10, 38].

The interaction potential (6) derived in the present paper is valid under assumption that only the lowest Landau level (lowest Fock–Darwin band) is occupied. The validity of this assumption for quantum systems confined in parabolic quantum dots has been checked and thoroughly discussed in [38] for $N = 2$, 3, and 4 electrons. This discussion [38] is based on comparison of the multicentre Hartree–Fock method [9, 10, 38] for the spin polarized electron system with the exact diagonalization method [38, 39] which assumes neither spin polarization nor the occupation of the lowest Landau level only. In the multicentre Hartree–Fock method [9, 10, 38] we construct the orthogonal one-electron wavefunctions as linear combinations of the N lowest Landau level wavefunctions (1) centred around different points and in the exact diagonalization method [38, 39] the basis set is taken in the form of Slater determinants built from several Fock–Darwin single-electron states. Let us briefly summarize the conclusions of this study [38]. The assumption that only the lowest Fock–Darwin band is occupied is not applicable for the ground states appearing in magnetic fields lower than those inducing MDD formation (these states correspond to the lowest Landau level filling factor $\nu > 1$ [8]). The fields inducing formation of the MDD phase for $N = 2$, 3, and 4 are equal to 1.75, 2.13, and 2.3 T [38] respectively. For the MDD ($\nu = 1$) and Wigner molecule states ($\nu < 1$) appearing for magnetic fields above the MDD decay one, the multicentre Hartree–Fock

method leads to a certain variational overestimation of the exact energy. This overestimation is largest in the MDD phase (about 0.5 meV for $N = 2$, 3, and 4) and tends to zero at the infinite magnetic field limit [38] as a linear function of $1/B$. The energy overestimation is partially due to a neglected admixture of the states belonging to higher Fock–Darwin bands with the ground state wavefunction. This admixture is provoked by the electron–electron interaction and is largest in the MDD state. In the multicentre Hartree–Fock method the electron–electron interaction takes on the maximum [10] value at the MDD breakdown: equal to 4.5, 10.8, and 19.4 meV for $N = 2$, 3, and 4 (the interaction energy per electron equals 2.25, 3.6, and 4.9 meV respectively). The overestimation of the total energy, which is only partially related to the neglected contribution of higher Fock–Darwin bands, is a few times smaller than the electron–electron interaction energy. Therefore, we conclude that the contributions of higher Fock–Darwin bands to the ground state are already of secondary importance for the MDD phase. For Wigner molecule states they are even smaller, since the principal effect of the Coulomb interaction in the Wigner localization regime is the separation of the electron charges, i.e., the Wigner crystallization itself. Higher Fock–Darwin bands are not necessary for its description. In [39] the size of the confined charge density calculated with the exact diagonalization method has been compared to the values given by the multicentre Hartree–Fock method (cf figure 9 of [39]) as a function of the external magnetic field for $N = 4$. The values obtained with the exact and approximate methods agree very well for the MDD state, for which the applicability of the lowest Landau level could be questioned. For higher states the multicentre Hartree–Fock method provides an average value around which the exact charge density radius oscillates [39]. These oscillations are due to the angular momentum transitions related to changes in occupation of the levels belonging to the lowest Fock–Darwin band [39]. References [38] and [39] show that in the MDD and Wigner crystallization regimes the contribution of higher Fock–Darwin bands leads only to secondary quantitative corrections to the properties of the ground state. On the basis of the above argumentation we conclude that the adopted assumption of the lowest Landau level (Fock–Darwin band) occupation is very well justified for the present qualitative considerations on states with $\nu \leqslant 1$, i.e. for the MDD and Wigner molecule states.

3. Results and discussion

In the present paper, we have used the simulated annealing Monte Carlo method in order to find both the global and local minima of the total potential energy (4) as functions of the external magnetic field.

The form of the interaction potential directly affects the total charge density. In figure 2, we illustrate this effect for the simplest case of the two-electron system. In the equilibrium configuration, the two electrons are situated at the ends of a line segment with the centre located at the origin, i.e., at the minimum of the external confinement potential. For low magnetic field ($B = 1.5$ T) the electron–electron interaction potential (6) is so soft near $R_{12} = 0$ that the equilibrium distance between the centres of the Gaussians (2) is equal to 0. For higher magnetic fields, the electron–electron interaction potential has a pronounced maximum for $R_{12} = 0$, which shifts the minimum of the total potential energy to the non-zero distance. We see that the repulsive core is formed in the total potential energy.

The equilibrium distance between the centres of electron localization (R_{12}) has been drawn in figure 3 for $N = 2$ as a function of the magnetic field. For $B \leqslant 1.81$ T the electrons are localized at the origin. For larger B the electrons become spatially separated and localized around different space sites. The equilibrium distance between the centres of electron localization passes through a maximum (at $B \simeq 6.5$ T) and then slowly decreases

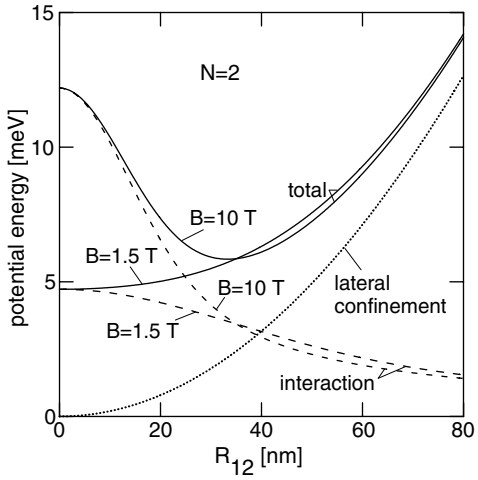

Figure 2. The total potential energy (solid curves), the electron–electron interaction potential energy (6) (dashed curves), and the lateral confinement potential energy (dotted curve) for the two-electron system as functions of the distance R_{12} between the centres of the Gaussians (2) for $B = 1.5$ and 10 T.

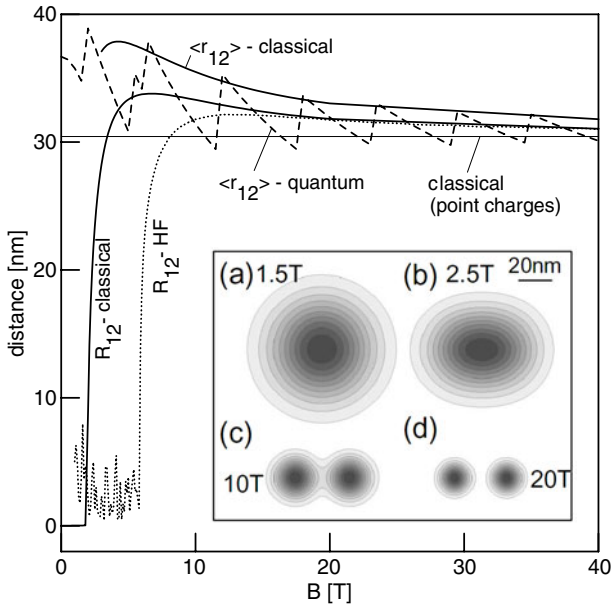

Figure 3. The equilibrium distance R_{12} between the centres of electron localization for $N = 2$ calculated using the present classical model (solid curve) and the Hartree–Fock results obtained with the multicentre basis (dotted curve) [9]. The horizontal thin line corresponds to the equilibrium distance between the point charges. The classical average electron–electron distance ($\langle r_{12} \rangle$) and its quantum average value obtained from the exact calculations (dashed line) are also shown. Inset: the charge density distribution on the x–y plane obtained by the classical approach for four magnetic fields. The darker the shade of grey, the larger the electron density.

toward $R_{12} = 30.44$ nm, which is the equilibrium distance in the system of two point charges. The growth of the equilibrium electron–electron distance above the value corresponding to

the point charges is related to the fact that—for the intermediate separations—the charges distributed according to the Gaussian function repel more strongly than the point charges (cf figure 1).

Figure 3 also displays the optimum value of the distance between the centres of electron localization (R_{12}) calculated with the multicentre Hartree–Fock method [9, 10]. According to the multicentre Hartree–Fock method [9], the MDD is created for $B < 5.9$ T. Figure 3 shows that in the MDD stability regime the optimum distance between the centres of wavefunctions (1) is close to zero. We note that—in the spin polarized quantum system—due to the antisymmetry of the spatial wavefunction, the distance between the centres of electron localization cannot fall to zero (that would result in the vanishing of the wavefunction).

Figure 3 shows that the magnetic field dependences of the distance between the centres of electron localization calculated in the framework of classical and quantum physics exhibit a remarkable similarity. According to the classical approach, at low magnetic fields, all the Gaussian charge density distributions are localized at the centre of the quantum dot. This phase is a classical counterpart of the quantum MDD phase [29]. The quantum MDD corresponds to the electrons occupying the energy levels with the subsequent angular momentum quantum numbers. The electron charge density of the MDD takes on the maximum value allowed by the Pauli exclusion principle and is squeezed around the centre of the quantum dot. In higher magnetic fields the MDD breaks down due to the rapidly growing interelectron repulsion which leads to the formation of a Wigner molecule with an island-like charge density distribution. The separation of the centres of electron localization is the classical analogue of the MDD decay. This effect appears abruptly at a certain magnetic field (cf figure 3). The breakdown of the MDD is predicted by the quantum calculations [9, 10] to occur at a higher magnetic field than that obtained in the present classical model, since the classical approach does not take into account the exchange interaction. The exchange interaction partly compensates the electron–electron Coulomb repulsion, but—due to its short range—disappears when the electron wavefunctions cease to overlap. In this way the exchange interaction stabilizes the MDD at the magnetic fields for which the classical model already predicts separation of the electrons.

In the infinite magnetic field limit, the present classical approach and the quantum Hartree–Fock method [9, 10] reproduce the same limit value of the equilibrium distance, which is characteristic for the point charge system. Figure 3 shows that for finite magnetic field, i.e., for $B \gtrsim 15$ T, the optimum distances between the centres of localization of the Gaussian charge density distribution, obtained from both the classical and the Hartree–Fock quantum calculations, have already become identical. This means that—in the high magnetic field regime—the Hartree–Fock results for the charge density distribution can be obtained from the present classical calculations.

The distance between the centres of electron localization is related to the average value of the electron–electron distance $\langle r_{12} \rangle$. In figure 3 we have compared the classical value of this quantity obtained by the present approach with the value obtained by the exact diagonalization of the two-electron Schrödinger equation (dashed curve in figure 3). The problem of two electrons can be separated into the equation for the centre-of-mass motion, which possesses an analytical solution, and the relative motion eigenproblem [12, 34]. The latter has been solved by a one-dimensional finite difference method. The quantum average value of the electron–electron distance exhibits cusps related to the stepwise increase of the angular momentum induced by the external magnetic field [8]. The classical value of the electron–electron distance is a smooth function decreasing slowly with the increasing magnetic field. The classical distance $\langle r_{12} \rangle$ provides an approximate upper bound for the quantum average value. In the infinite magnetic field limit, all the distances presented in figure 3 tend to the equilibrium distance between the classical point charges.

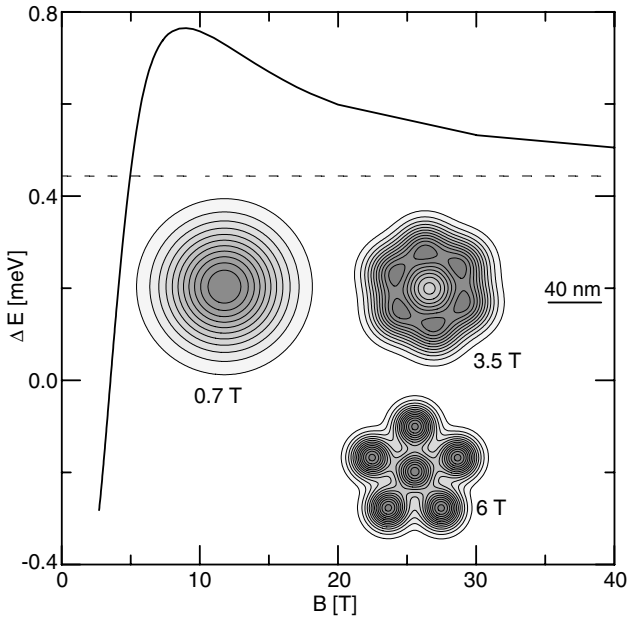

Figure 4. The difference ΔE in total potential energy between the 0–6 and 1–5 Wigner molecule isomers as a function of external magnetic field B. The horizontal dashed line shows the corresponding energy difference for the point charges. Inset: charge density contours for the lowest energy configuration for $B = 0.7$ T (the counterpart of the MDD), 3.5 T (0–6 isomer), and 6 T (1–5 isomer).

The inset of figure 3 shows the charge density contours obtained with the present classical approach. Plot (a) for $B = 1.5$ T corresponds to the classical counterpart of the MDD, for which the electrons are localized at the origin. In plot (b) (for $B = 2.5$ T) the centres of electron localization become separated; the charge density distribution loses its cylindrical symmetry and is elliptically deformed. Plots (c) and (d) show the distinct separation of the electron charges characteristic of the Wigner molecule.

The system of six point charges possesses two stable isomers, which are close in energy [18–20]. The lowest energy isomer corresponds to the configuration with one electron situated at the centre and five others forming a pentagon surrounding it. In the metastable isomer the electrons form a hexagon. Generally, in the equilibrium configurations, the electrons form concentric rings [18, 19]. In the present paper we label the isomer of the Wigner molecule giving the numbers of electrons in the subsequent rings starting from the innermost one. For example, for the system of six point charges the lowest energy isomer is denoted by 1–5 and the metastable isomer by 0–6. Figure 4 depicts the energy difference of two six-electron isomers as a function of the external magnetic field. In contrast to the case for the point charge system, in the present model with the spread-out charge distribution the 0–6 isomer possesses a lower energy than the 1–5 isomer for $B < 3.53$ T. For higher magnetic fields the 1–5 isomer becomes the most stable. Figure 4 shows that the energy difference passes through a maximum for $B = 9$ T and then decreases toward $\Delta E = 0.444$ meV, which corresponds to the point charge system.

In the magnetic field regime above the MDD breakdown, the interaction between the nearest neighbours in the Wigner molecule is stronger than the interaction between the point charges (cf figure 1), which changes the shape of the lowest energy configuration in comparison to that of the point charge system in finite magnetic fields. The system of spread-out charges

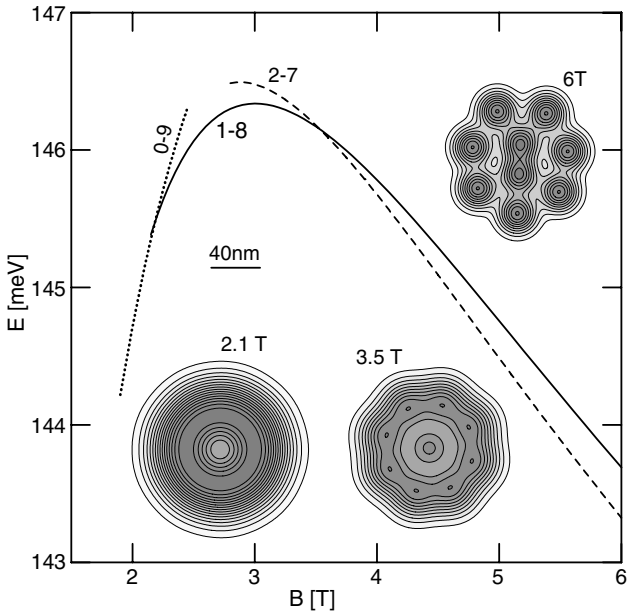

Figure 5. The total potential energy E of the nine-electron Wigner molecule isomers 0–9 (dotted curve), 1–8 (solid curve), and 2–7 (dashed curve) as a function of external magnetic field B. Inset: charge density contours for the most stable isomers for $B = 2.1$ T (0–9), $B = 3.5$ T (1–8), and $B = 6$ T (2–7).

tends to minimize the number of nearest neighbours. Therefore, after the MDD breakdown, the lowest energy isomer corresponds to the centres of electron localization located on a single ring. In this configuration, the number of nearest neighbours is minimal but also the distances between them are smaller than in the other metastable configurations. The small distances become energetically less favourable for higher magnetic fields, for which the electrostatic interaction between the Gaussian charge densities tends to the Coulomb interaction (cf figure 1). This modification of the interaction triggers the transitions between the different configurations of the Wigner molecule (cf figure 4).

Figure 5 shows the results for the nine-electron system. After the MDD breakdown (at $B = 0.75$ T), the 0–9 isomer is the most stable one. This is the only stable nine-electron isomer in the low magnetic field regime. The other metastable isomers, i.e., 1–8 and 2–7, appear at $B = 2.15$ and 2.8 T and become the most stable at $B = 2.2$ and 3.55 T, respectively. The inset of figure 5 depicts the charge density contours for the most stable nine-electron isomers. We note that the 0–9 isomer for $B = 2.1$ T exhibits nearly perfect circular symmetry with the minimum of the charge density located at the centre.

We have obtained similar transformations of the lowest energy isomers for all the Wigner molecules consisting of more than five electrons. The present results are summarized in figure 6, which shows the phase diagram for the Wigner molecules with $N = 2, \ldots, 20$ as a function of the external magnetic field. We see that the magnetic field which induces the MDD breakdown decreases with the increasing number of electrons, which is related to the increasing contribution of the electron–electron interaction. For $N = 2, \ldots, 5$ the only transformation of the lowest energy configuration is related to the MDD breakdown. For the point charge systems with $N = 6$, 7, and 8 the lowest energy configurations are composed of two rings each with one electron in the centre and the others forming polygons around it [18, 19]. Figure 6 shows

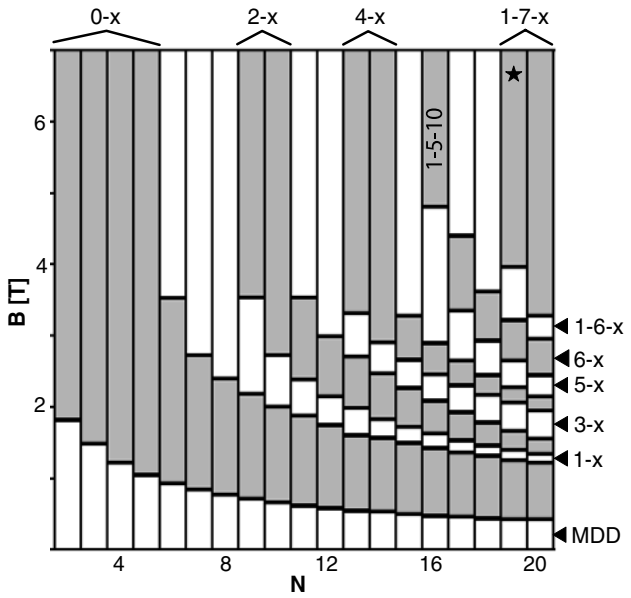

Figure 6. A phase diagram showing the lowest energy isomers of the Wigner molecules as a function of magnetic field B and number of electrons N. The number of electrons on the outermost ring is denoted by x. The subsequent grey and white areas correspond to the same number of electrons on the inner ring (the only exception of the 1–5–10 isomer is given explicitly). $\star$: the lowest energy isomer 1–6–12 of the 19-electron Wigner molecule is created at $B = 10.5$ T.

that—in the Wigner molecules with the spread-out charge density—the other stable isomers are obtained for $N = 6$, 7, and 8 just after the MDD breakdown. These isomers consist of a single ring. For $N = 9, \ldots, 15$ the point charge systems in equilibrium are composed of two rings with 2, 3, 4, or 5 electrons on the inner ring [19]. For the Gaussian charge density the electrons enter the central ring one by one as the external magnetic field increases. Similar effects appear for larger numbers of electrons, i.e., for $N = 16, \ldots, 20$, which—in the high magnetic field limit—produce three-ring isomers each with a single electron located at the centre. The phase diagram presented in figure 6 exhibits a clear regularity in both the sequence of the lowest energy isomers and the magnetic fields which induce the equivalent transformations for the different numbers of electrons. In particular, figure 6 shows that the magnetic field which induces the entrance of the subsequent electrons into the inner ring is a monotonically decreasing function of N.

The classical phase diagram (figure 6) shows that—for $N \geqslant 6$—the intermediate phases of the Wigner molecules appear in the magnetic field regime between the MDD breakdown and the infinite field limit. The present prediction of the existence of the different classical Wigner molecule phases is in agreement with the results of the quantum calculations [8, 9, 31, 32]. For $N \geqslant 6$ after the MDD breakdown the electrons prefer to occupy the outer rings and enter the inner rings at higher magnetic fields. This property is also the most characteristic feature of the phase diagram for the quantum Wigner molecules obtained by Szafran *et al* [9].

According to figure 2 the size of the Wigner molecule depends on the external magnetic field. This dependence is related to the modification of the interaction potential by the external magnetic field. We have found that not only is the size of the molecule modified, but also the shape of some isomers is changed by the external magnetic field. The corresponding changes of the size and shape are illustrated in figure 7 for the six-electron system.

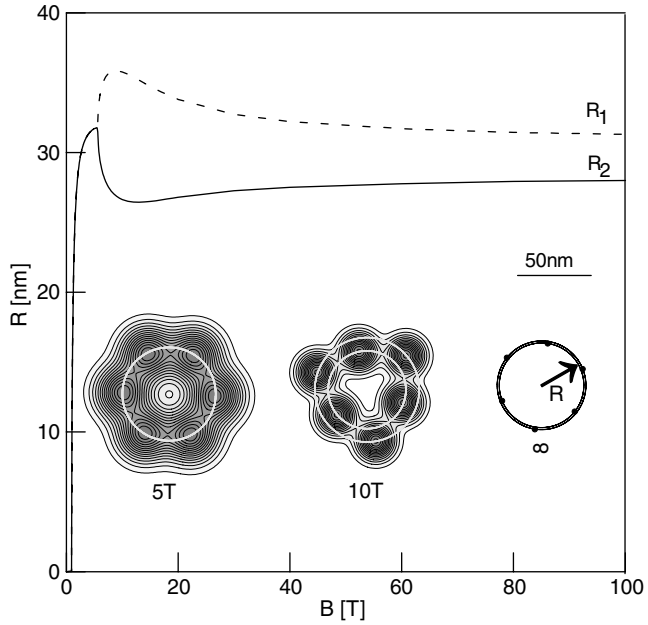

Figure 7. Distances R_1 and R_2 of the two electrons from the centre of the quantum dot as functions of magnetic field B for the 0–6 isomer. Inset: charge density contours for $B = 5$ and 10 T and for $B \longrightarrow \infty$. The rings on which the centres of the electron charge density are located are marked by the circles.

In the 0–6 isomer of the point charge system (cf figure 7 for $B \longrightarrow \infty$) the electrons are situated on two concentric rings with different radii. In the system with the Gaussian charge density distribution, this feature is also obtained at lower magnetic fields (cf the inset of figure 7). The corresponding radii of the two rings are equal for $B < 5.5$ T. Then, the centres of electron localization form a perfectly regular hegaxon. This hexagonal shape occurs in the range of the magnetic field for which the 0–6 isomer is the most stable, i.e., $B \in (0.93, 3.52)$ T. Figure 7 shows that for $B = 5.5$ T the radii of the rings split as functions of the magnetic field. At the magnetic field which corresponds to this splitting, the 1–5 isomer is already the most stable (cf figure 4). The difference between the outer ring and inner ring radii is the largest for $B = 10$ T. If the magnetic field increases further, both the radii approach the infinite magnetic field limit values $R_1 = 30.3$ nm and $R_2 = 28.9$ nm. We see that for $B = 10$ T, i.e., for the maximal value of the difference between the radii, the shape of 0–6 isomer significantly differs from both the regular hegaxon and the stable point charge configuration. In the recent work of Reusch and Grabert [5], the authors calculated the charge density for the 0–6 isomer (cf figure 14(f) in [5]) by the unrestricted Hartree–Fock method. This plot [5] has been obtained for a relatively low magnetic field, for which isomers 0–6 and 1–5 possess almost degenerate energies. At this magnetic field, the centres of electron localization form a perfectly regular hegaxon [5], which is in agreement with the present classical results (cf figure 7).

In figure 8 we plot the charge density for the 1–8 isomer of the nine-electron molecule for different magnetic fields. For $B = 5$ T the electrons on the outer ring are situated at equal distances from the central electron. However, for larger magnetic field the outer ring splits into two concentric circles. The difference of the radii of these circles is maximal for $B = 11.8$ T and converges to 0.4 nm if $B \longrightarrow \infty$.

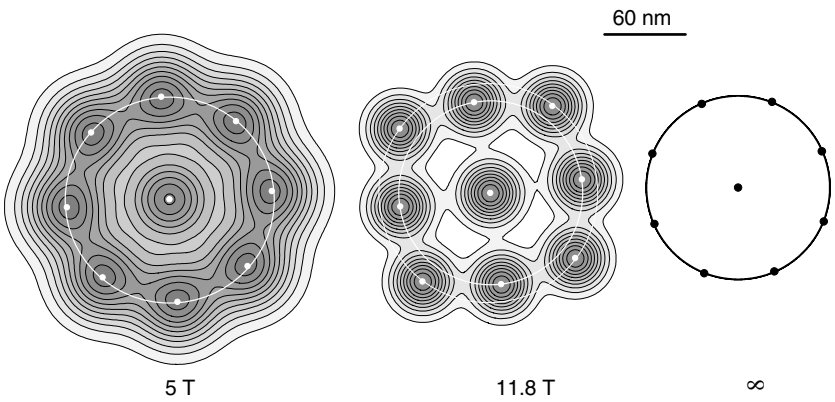

Figure 8. Charge density contours for the nine-electron Wigner molecule isomer 1–8 for $B = 5$ and 11.8 T and for $B \longrightarrow \infty$. Dots show the centres of the electron localization and circles, the corresponding rings.

Figures 7 and 8 show that the shape of certain isomers of the Wigner molecules strongly depends on the external magnetic field. In a recent study of the quantum phase diagram for Wigner molecules, Szafran *et al* [9, 10] assumed that the shape of the quantum isomer is obtained by a uniform scaling of the corresponding classical configuration. The results of figures 7 and 8 indicate that application of a non-uniform scaling is also possible, at least for some isomers. In particular, for $N = 6$ the non-uniform scaling should lead to the extension of the estimated [9] magnetic field regime in which the ground state corresponds to the 0–6 configuration. This results from the present finding that the 1–5 isomer conserves its shape on changing the magnetic field, but the shape of the 0–6 isomer is considerably modified (cf figure 7).

In the infinite magnetic field limit the multicentre Hartree–Fock method reproduces the lowest energy classical configurations of point charges [10]. The error of the energy estimate obtained with a semiclassical charge distribution tends to zero at the infinite magnetic field limit [38]. Taking into account the finite spread of the electron charges gives a reasonable quantitative agreement of the present classical model and quantum calculations for finite magnetic fields. For two-electron systems this agreement is reached for $B \gtrsim 10$ T (cf figure 3). For lower magnetic fields the present model is still qualitatively applicable for spin polarized MDD and Wigner molecule states. However, it does not provide classical counterparts for quantum ground states with $\nu > 1$ appearing at magnetic fields below that for the MDD formation.

4. Conclusions and summary

We have studied the classical features of the magnetic field-induced Wigner crystallization in electron systems confined within quantum dots. The present study is performed in the framework of classical physics and is based on the assumption that the charge density associated with each electron can be identified with the charge density of the electron occupying the lowest Landau level. This approach allows us to simulate a number of interesting effects which were previously obtained in quantum calculations. In particular, we have obtained the classical counterpart of the quantum MDD phase and the MDD breakdown into a Wigner molecule. The semiclassical character of the quantum Wigner phases is a fairly well known

feature. However, the present finding, that the classical model reproduces the MDD phase, is an unexpected result.

Moreover, we have found the phase transitions between different isomers of the Wigner molecules, which are in qualitative agreement with the previous quantum results. We have shown that not only the high magnetic field behaviour, but also the other characteristic properties of the quantum systems can be obtained within the present classical model.

Acknowledgment

This work was supported by the Polish Government Scientific Research Committee (KBN).

References

[1] Wigner E P 1934 *Phys. Rev.* **46** 1002
[2] Müller H-M and Koonin S E 1996 *Phys. Rev.* B **54** 14532
[3] Yannouleas C and Landman U 2000 *Phys. Rev.* B **61** 15895
[4] Yannouleas C and Landman U 2002 *Phys. Rev.* B **66** 115315
[5] Reusch B and Grabert H 2003 *Phys. Rev.* B **68** 045309
[6] Kainz J, Mikhailov S A, Wensauer A and Rössler U 2002 *Phys. Rev.* B **65** 115305
[7] Reimann S M, Koskinen M, Manninen M and Mottelson B R 1999 *Phys. Rev. Lett.* **83** 3270
[8] Reimann S M and Manninen M 2002 *Rev. Mod. Phys.* **74** 1283
[9] Szafran B, Bednarek S and Adamowski J 2003 *Phys. Rev.* B **67** 045311
Szafran B, Bednarek S and Adamowski J 2003 *Phys. Rev.* B **67** 159902 (erratum)
[10] Szafran B, Bednarek S and Adamowski J 2003 *J. Phys.: Condens. Matter* 4189
[11] Szafran B, Bednarek S and Adamowski J 2003 *Phys. Rev.* B **67** 115323
[12] Matulis A and Peeters F M 2001 *Solid State Commun.* **117** 655
[13] Maksym P A, Immamura H, Mallon G P and Aoki H 2000 *J. Phys.: Condens. Matter* **12** R299
[14] Egger R, Häusler W, Mak C H and Grabert H 1999 *Phys. Rev. Lett.* **82** 3320
[15] Akbar S and Lee I-H 2001 *Phys. Rev.* B **63** 165301
[16] Mikhailov S A and Ziegler K 2002 *Eur. Phys. J.* B **28** 117
[17] Nemeth Z A and Pichard J-L 2002 *Europhys. Lett.* **58** 744
[18] Bolton F and Rössler U 1993 *Superlatt. Microstruct.* **13** 139
[19] Bedanov V M and Peeters F M 1994 *Phys. Rev.* B **49** 2667
[20] Partoens B and Peeters F M 1994 *J. Phys.: Condens. Matter* **9** 5383
[21] Schweigert V A and Peeters F M 1995 *Phys. Rev.* B **51** 7700
[22] Candido L, Rino J P, Studuart N and Peeters F M 1998 *J. Phys.: Condens. Matter* **10** 11627
[23] Ying-Jui Lai and Lin I 1999 *Phys. Rev.* E **60** 4743
[24] Cornelissens Y G, Partoens B and Peeters F M 2000 *Physica* E **8** 314
[25] Kong M, Partoens B and Peeters F M 2002 *Phys. Rev.* E **65** 046602
[26] Muto S and Aoki H 2000 *Physica* E **6** 116
[27] Marlo M, Alatalo M, Harju A and Nieminen R M 2002 *Phys. Rev.* B **66** 155322
[28] Saint Jean M, Even C and Guthmann C 2001 *Europhys. Lett.* **55** 45
[29] MacDonald A H, Yang S R E and Johnson M D 1993 *Aust. J. Phys.* **46** 345
[30] Eto M 1997 *Japan. J. Appl. Phys.* **36** 3924
[31] Manninen M, Viefers S, Koskinen M and Reimann S M 2001 *Phys. Rev.* B **64** 245322
[32] Yang S R E and MacDonald A H 2002 *Phys. Rev.* B **66** 041304
[33] Mikhailov S A and Savostianova N A 2002 *Phys. Rev.* B **66** 033307
[34] Dineykhan M and Nazmitdinov R G 1999 *J. Phys.: Condens. Matter* **11** L83
[35] Oosterkamp T H, Janssen J W, Kouwenhoven L P, Austing D G, Honda T and Tarucha S 1999 *Phys. Rev. Lett.* **82** 2931
[36] Taut M 1993 *Phys. Rev.* A **48** 3561
[37] Polini M, Moulopolous K, Davoudi B and Tosi M P 2002 *Phys. Rev.* B **65** 165306
[38] Szafran B, Bednarek S, Adamowski J, Tavernier M B, Anisimovas E and Peeters F M 2003 *Eur. Phys. J.* D 10.1140/epjd/e2003-00320-5
(Szafran B, Bednarek S, Adamowski J, Tavernier M B, Anisimovas E and Peeters F M 2003 *Preprint* cond-mat/0310172)
[39] Tavernier M B, Anisimovas E, Peeters F M, Szafran B, Adamowski J and Bednarek S 2003 *Phys. Rev.* B **68** 205305